Langmuir

Article

pubs.acs.org/Langmuir

Cation Alkyl Side Chain Length and Symmetry Effects on the Surface Tension of Ionic Liquids

Hugo F. D. Almeida,[†] Mara G. Freire,[†] Ana M. Fernandes,[‡] José A. Lopes-da-Silva,[‡] Pedro Morgado,[§] Karina Shimizu,[§] Eduardo J. M. Filipe,[§] José N. Canongia Lopes,[§,⊥] Luís M. N. B. F. Santos,[#] and João A. P. Coutinho*,[†]

[†]Departamento de Química, CICECO, Universidade de Aveiro, 3810-193 Aveiro, Portugal

[‡]QOPNA Unit, Departamento de Química, Universidade de Aveiro, 3810-193 Aveiro, Portugal

[§]Centro de Química Estrutural, Instituto Superior Técnico, Universidade de Lisboa, Av. Rovisco Pais, 1049-001 Lisboa, Portugal

[⊥]Instituto de Tecnologia Química e Biológica, Universidade Nova de Lisboa, Avenida da República, 2750-154 Oeiras, Portugal

[#]Centro de Investigação em Química, Departamento de Química e Bioquímica, Faculdade de Ciências, Universidade do Porto, Rua do Campo Alegre, 687, 4169-007 Porto, Portugal

Supporting Information

ABSTRACT: Aiming at providing a comprehensive study of the influence of the cation symmetry and alkyl side chain length on the surface tension and surface organization of ionic liquids (ILs), this work addresses the experimental measurements of the surface tension of two extended series of ILs, namely R,R′-dialkylimidazolium bis[(trifluoromethyl)sulfonyl]imide ($[C_nC_n\text{im}][NTf_2]$) and R-alkyl-3-methylimidazolium bis[(trifluoromethyl)sulfonyl]imide ($[C_nC_1\text{im}][NTf_2]$), and their dependence with temperature (from 298 to 343 K). For both series of ILs the surface tension decreases with an increase in the cation side alkyl chain length up to aliphatic chains no longer than hexyl, here labeled as critical alkyl chain length (CACL). For ILs with aliphatic moieties longer than CACL the surface tension displays an almost constant value up to $[C_{12}C_{12}\text{im}][NTf_2]$ or $[C_{16}C_1\text{im}][NTf_2]$. These constant values further converge to the surface tension of long chain *n*-alkanes, indicating that, for sufficiently long alkyl side chains, the surface ordering is strongly dominated by the aliphatic tails present in the IL. The enthalpies and entropies of surface were also derived and the critical temperatures were estimated from the experimental data. The trend of the derived thermodynamic properties highlights the effect of the structural organization of the IL at the surface with visible trend shifts occurring at a well-defined CACL in both symmetric and asymmetric series of ILs. Finally, the structure of a long-alkyl side chain IL at the vacuum-liquid interface was also explored using Molecular Dynamics simulations. In general, it was found that for the symmetric series of ILs, at the outermost polar layers, more cations point one of their aliphatic tails outward and the other inward, relative to the surface, than cations pointing both tails outward. The number of the former, while being the preferred conformation, exceeds the latter by around 75%.

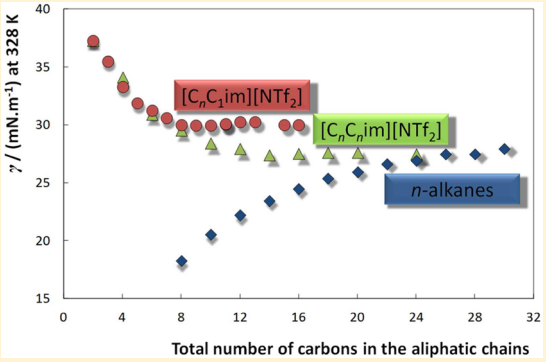

INTRODUCTION

Ionic liquids (ILs) are generally defined as salts presenting a melting temperature below 373 K; yet, a vast number of compounds are liquid at temperatures close to room temperature.[1] Furthermore, most ILs display other peculiar properties, namely a negligible vapor pressure, a high ionic conductivity, nonflammability, high thermal and chemical stabilities, and an improved solvation ability for a large range of compounds.[2−6] Because of these features, during the past decade, ILs were extensively explored as major alternatives to traditional solvents and have been the object of various industrial applications.[7] Because of their structural variety, there is also a considerable number of different ILs resulting from the combination of diverse cations and anions and which allows their design for particular applications.

The major applications regarding ILs often involve the presence of a second liquid or gas phase where the interface among the fluids plays an important role.[2,7] As a result, the knowledge of the interfacial properties of ILs, namely their surface (air−liquid) and interfacial (liquid−liquid) tensions, and the correlation of these properties with their chemical structure, are essential requirements for choosing a given fluid for a specific task. Besides the characterization of their thermophysical properties, the knowledge of the interactions that occur at the bulk and the interfacial phenomena with the surrounding medium are of main importance. According to the

Received: October 10, 2013
Revised: May 15, 2014
Published: May 16, 2014

Langmuir's principle of independent surface action, each molecule present at the interface contributes with free surface energy to the surface tension of the liquid, and this principle has shown to be also applicable to ILs.[8,9]

Compared to more recurrent thermophysical properties, such as density and viscosity, the surface tensions of ILs are a less studied field. Consistent and accurate measurements of surface tensions of ILs are not easy because of the presence of surface-active impurities, which usually lead to large deviations in the respective values and between different authors.[10] Moreover, ILs are highly hygroscopic and the control of their water content at low values is a major drawback in accurate surface tension measurements. A recent review[10] regarding the surface tension of ILs and their solutions critically addressed these issues and the major sources of error in the experimental assays.

General trends on the surface tension values according to the IL chemical structure have been provided and discussed.[10] However, the "designer solvent" feature of ILs does not solely result from the ability of combining a wide range of substantially different cations and anions. In fact, the isomerism of the cation also plays a considerable role in the thermophysical properties and liquid−liquid phase behavior of systems involving ILs.[11,12] In addition, the cation symmetry and the cation side alkyl chain length have shown to influence the densities and viscosities of ILs.[13] Depending on the property under measurement, the influence of the cation symmetry and alkyl side chain length can be of high importance or of a more subtle character.[13] Small-wide angle X-ray scattering (SWAXS) patterns at ambient conditions were determined and analyzed for both asymmetric and symmetric series of imidazolium-based ILs.[13] The gathered data revealed that both asymmetric and symmetric members are characterized by the occurrence of a distinct degree of mesoscopic structural organization above a given threshold in the side alkyl chain length and by a different degree of interdigitation of the aliphatic tails in the two families.[13] Nevertheless, an extended study on the surface tensions as a function of the cation alkyl side chain length and on the influence of the cation symmetry, achieved by dissubstituted cations with aliphatic tails of similar length, in parallel with their nanostructuration evaluation, has not been attempted yet.

To address both the effects of the cation alkyl side chain length and symmetry upon the surface ordering in ILs, we measured and are reported novel surface tension data between (298.2 and 343.2) K for 17 compounds. This analysis is possible because of the chosen ILs: R,R′-dialkylimidazolium bis[(trifluoromethyl)sulfonyl]imide (symmetric series) and R-alkyl-3-methylimidazolium bis[(trifluoromethyl)sulfonyl]imide (asymmetric series). Electrospray ionization mass spectrometry data were further used to gather additional insights into the interpretation of the surface tension results in terms of the ILs' interaction energies. Molecular Dynamics simulation was also used to corroborate the experimental surface tension results and surface organization. The relationship between the surface tension of ILs and their molar volumes was also explored. Furthermore, the related surface thermodynamic functions, such as surface entropy and surface enthalpy, were determined. The hypothetical critical temperatures of the ILs investigated were also estimated. In summary, novel evidence regarding the comparison between the surface tension and estimated properties behavior of R,R′-dialkylimidazolium- and R-alkyl-3-methylimidazolium-based ILs are presented and compared against that of *n*-alkanes of equivalent alkyl chain length.

EXPERIMENTAL SECTION

Materials. Seventeen bis[(trifluoromethyl)sulfonyl]imide-based ILs were studied in this work. The symmetric series of bis[(trifluoromethyl)sulfonyl]imide-based ILs, $[C_nC_n\text{im}][NTf_2]$, comprises the cations 1,3-dimethylimidazolium ($[C_1C_1\text{im}][NTf_2]$), 1,3-diethylimidazolium ($[C_2C_2\text{im}][NTf_2]$), 1,3-dipropylimidazolium ($[C_3C_3\text{im}][NTf_2]$), 1,3-dibutylimidazolium ($[C_4C_4\text{im}][NTf_2]$), 1,3-dipentylimidazolium ($[C_5C_5\text{im}][NTf_2]$), 1,3-dihexylimidazolium ($[C_6C_6\text{im}][NTf_2]$), 1,3-diheptylimidazolium ($[C_7C_7\text{im}][NTf_2]$), 1,3-dioctylimidazolium ($[C_8C_8\text{im}][NTf_2]$), 1,3-dinonylimidazolium ($[C_9C_9\text{im}][NTf_2]$), 1,3-didecylimidazolium ($[C_{10}C_{10}\text{im}][NTf_2]$), and 1,3-didodecylimidazolium ($[C_{12}C_{12}\text{im}][NTf_2]$). The asymmetric family of bis[(trifluoromethyl)sulfonyl]imide-based ILs, $[C_nC_1\text{im}][NTf_2]$, includes the cations 1-methyl-3-nonylimidazolium ($[C_9C_1\text{im}][NTf_2]$), 1-decyl-3-methylimidazolium ($[C_{10}C_1\text{im}][NTf_2]$), 1-methyl-3-undecylimidazolium ($[C_{11}C_1\text{im}][NTf_2]$), 1-dodecyl-3-methylimidazolium ($[C_{12}C_1\text{im}][NTf_2]$), 1-methyl-3-tetradecylimidazolium ($[C_{14}C_1\text{im}][NTf_2]$), and 1-hexadecyl-3-methylimidazolium ($[C_{16}C_1\text{im}][NTf_2]$). All ILs were supplied by Iolitec with purities ≥99 wt %. The general ionic structures of the studied compounds are depicted in Figure 1.

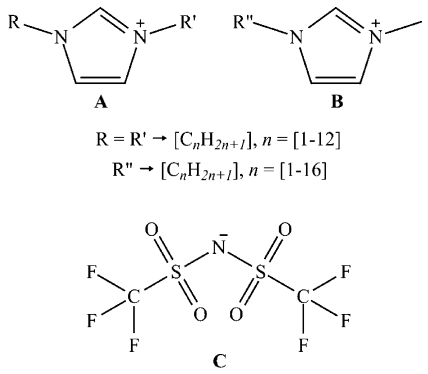

Figure 1. Ionic structures of (A) R,R′-dialkylimidazolium cation ($[C_nC_n\text{im}]^+$), (B) R-alkyl-3-methylimidazolium cation ($[C_nC_1\text{im}]^+$), and (C) bis[(trifluoromethyl)sulfonyl]imide anion ($[NTf_2]^-$).

To remove traces of water and volatile compounds from ILs, we dried individual samples at moderate temperature (≈ 323 K) and at high vacuum (≈1 × 10^{-5} Pa), under constant stirring, and for a minimum period of 48 h. After this purification step, the purity of all ILs was further checked by ^{1}H, ^{13}C and ^{19}F NMR. Furthermore, the water content of each IL, after the drying step and immediately before the measurements of the surface tensions, was determined by Karl Fischer titration using a Metrohm 831 Karl Fischer coulometer. The reagent employed was Hydranal-Coulomat AG from Riedel-de Haën. The water content in each IL is presented in Table SI.1 in the Supporting Information with a maximum water content of 0.051 wt %.

Experimental Procedure. The surface tension of each sample was determined by the analysis of the shape of a pendant drop and measured using a Dataphysics (model OCA-20) contact angle system. Drop volumes of (10 ± 1) μL were obtained using a Hamilton DS 500/GT syringe connected to a Teflon coated needle placed inside an aluminum air chamber able to maintain the temperature of interest within ±0.1 K. The surface tension measurements were performed in the temperature range from 298.2 to 343.2 K, with the exception of $[C_{12}C_{12}\text{im}][NTf_2]$, $[C_{14}C_1\text{im}][NTf_2]$ and $[C_{16}C_1\text{im}][NTf_2]$, performed in the temperature range from 328.2 to 343.2 K, due to their higher melting temperatures. The temperature inside the aluminum chamber in which the surface tensions were determined was measured with a Pt100 within ±0.1 K (placed at a distance of approximately 20 mm from the liquid drop). After reaching a specific temperature inside the aluminum chamber, the measurements were

dx.doi.org/10.1021/la501308q | *Langmuir* 2014, 30, 6408−6418

carried out after 30 min to guarantee the thermal stabilization. Silica gel was kept inside the air chamber aiming at keeping a dry environment.

For the surface tensions determination at each temperature, and for each IL, at least 4 drops were formed and analyzed. For each drop, an average of 200 images was captured. The analysis of the drop shape was done with the software modules SCA 20 where the gravitational acceleration (g = 9.8018 m·s^2) and latitude (lat = 40°) were used according to the location of the assay. The density values required for the calculation of the surface tensions from the drop image data were taken from literature.[13] Further details on the equipment and its validity to measure surface tensions of ILs were previously addressed.[14]

Electrospray ionization mass spectra (ESI-MS) were acquired with a Micromass Q-Tof 2 (Micromass, Manchester, UK), operating in the positive ion mode, equipped with a Z-spray source. Source and desolvation temperatures were 353 and 373 K, respectively. IL solutions in methanol, at concentrations circa to 1 × 10^{-4} mol L^{-1}, were introduced at a 10 μL·min^{-1} flow rate. The capillary and the cone voltage were 2600 V (or 3000 V) and 30 V, respectively. Nitrogen was used as nebulization gas and argon as collision gas.

ESI-MS-MS spectra were acquired by selecting the precursor ion with the quadrupole, and performing collisions with argon at variable energies in the hexapole. The laboratory frame collision energy (E_{Lab}) can be changed and is reflected by a variation in the collision energy fraction that is actually converted to the ions' internal energy. The variable collisions energies in the ESI-MS-MS spectra are taken from the relative abundances of precursor and fragment ions, whereas the energy values corresponding to a relative abundance of the precursor ion of 50% ($E_{Lab,1/2}$) are here used as a measure of the relative dissociation energy. In this inelastic collision of the projectile ion with the target neutral, the total available energy for conversion of translational (or kinetic) to internal (or vibrational) energy of the projectile ion is the center of mass energy (E_{cm}), which can be calculated from E_{Lab}, and from the masses of the neutral target and precursor ion. The calculated dissociation energies from the experimental E_{Lab} values represent the energy required to separate a cation from the neutral IL in the gas phase and, as such, can be considered a good approximation to the cation−anion relative interaction energy. This method has already proved to be an adequate strategy in the study of the relative cation−anion interaction strength in ILs.[15] Further details can be found elsewhere.[15] Triplicate measurements were performed for each selected precursor ion and standard deviations varying between 0.3 and 5% were obtained.

Molecular Dynamics Simulations. The interfacial structure of [$C_{10}C_{10}$im][NTf_2] was also studied using molecular dynamics (MD) simulations based on the CL&P all-atom force field.[16,17] All simulation runs were performed using the DL_POLY 2.20 simulation package.[18]

The starting point for the different MD studies was a low-density configuration consisting of 300 ionic pairs placed in a cubic box with 13 nm sides. This system underwent an equilibration process under isobaric isothermal ensemble conditions with p = 0.1 MPa and T = 400 K (Nosé−Hoover thermostats and barostats with relaxation time constants of 1 and 4 ps, respectively), a 2 fs time-step, and cutoff distances of 1.2 nm (Ewald corrections and tail corrections were used beyond such distances). After 1.3 ns the density of the system reached constant and consistent values, indicating that equilibrium had been attained and possible ergodicity problems had been overcome. Finally, four consecutive production stages of 1.0 ns each were performed with cutoff distances of 2 nm and the combined results were used for the evaluation of relevant structural data in bulk [$C_{10}C_{10}$im][NTf_2]. The final length of the cubic box sides was approximately 6.6 nm.

To model the IL-vacuum interface, the simulation box containing the pure IL was expanded to a value three times its initial size by elongating the sides of the cube along the z-axis. This generated an IL slab with two explicit liquid-vacuum interfaces and a 6.6 nm thickness inside a quadrangular-prism box with a length of 19.8 nm and a 6.6 × 6.6 nm base. A simulation run was then conducted under NVT ensemble conditions (T = 500 K), with 0.5 and 2 ns equilibration and production stages, respectively; no drift in the studied properties was found from block analysis of the production stage. In order to obtain a thicker IL slab, the system was then subjected to a lateral compression (in the x- and y-axes) by running a NpT ensemble simulation for around 150 ps. This process leads to a prismatic box with a 5.2 × 5.2 nm base and a liquid layer about 10 nm thick. This configuration was then subjected to new (0.5 ns equilibration + 2 ns production) processes under NVT conditions that conducted to the results discussed below. Possible ergodicity problems were tested by calculating the system properties at different stages of the production runs, including comparisons between slabs of different thickness or between processes interspersed by temperature-annealing cycles.

It should be remarked that, in this work, no surface tension results were calculated by MD simulation. Only the surface structure of the ILs is analyzed by MD simulation results.

RESULTS AND DISCUSSION

The surface tension values for the bis[(trifluoromethyl)-sulfonyl]imide-based ILs measured in this work are reported in Table SI.2 in the Supporting Information. For a more detailed analysis on the dependence of the surface tension with temperature as well as among different ILs, the obtained results are depicted in Figures 2 and 3, for R,R′-dialkylimidazolium bis[(trifluoromethyl)sulfonyl]imide ([$C_nC_n$im][NTf_2]) and for R-alkyl-3-methylimidazolium bis[(trifluoromethyl)sulfonyl]-imide ([$C_nC_1$im][NTf_2]) ILs, respectively.

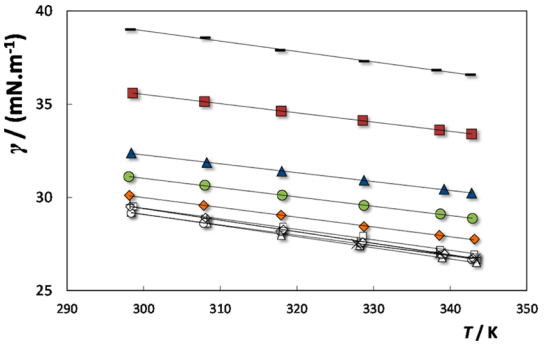

Figure 2. Surface tension values for the [$C_nC_n$im][NTf_2] ILs as a function of temperature: black bar, [C_1C_1im][NTf_2]; red square, [C_2C_2im][NTf_2]; blue triangle, [C_3C_3im][NTf_2]; green circle, [C_4C_4im][NTf_2]; orange diamond, [C_5C_5im][NTf_2]; white square, [C_6C_6im][NTf_2]; white triangle, [C_7C_7im][NTf_2]; white circle, [C_8C_8im][NTf_2]; white diamond, [C_9C_9im][NTf_2]; +, [$C_{10}C_{10}$im]-[NTf_2]; ×, [$C_{12}C_{12}$im][NTf_2].

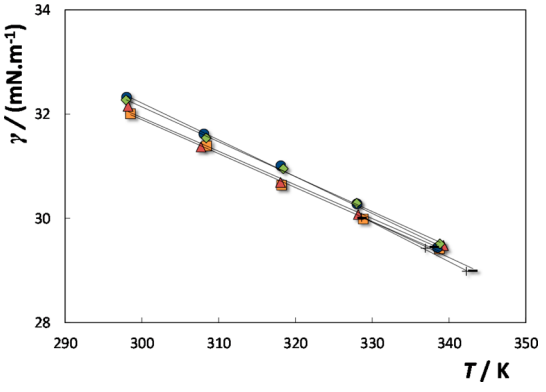

Figure 3. Surface tension values for the [$C_nC_1$im][NTf_2] ILs as a function of temperature: orange square, [C_9C_1im][NTf_2]; red triangle, [$C_{10}C_1$im][NTf_2]; blue circle, [$C_{11}C_1$im][NTf_2]; green diamond, [$C_{12}C_1$im][NTf_2]; black bar, [$C_{14}C_1$im][NTf_2]; +, [$C_{16}C_1$im][NTf_2].

dx.doi.org/10.1021/la501308q | Langmuir 2014, 30, 6408−6418

Most data available in literature correspond to $[C_nC_1im][NTf_2]$ ILs[8,19−21] whereas results for symmetric ILs of the type $[C_nC_nim][NTf_2]$ are particularly scarce.[8,21] The average relative deviation between the data collected in this work and those reported for $[C_{10}C_1im][NTf_2]$ is 7%.[19−21] However, a good agreement (average relative deviation of 1%) is observed between the data gathered in this work compared to those previously published by Carvalho et al.[21] and using a different technique. For $[C_{12}C_1im][NTf_2]$ and $[C_{14}C_1im][NTf_2]$ the average relative deviations between our data and literature results are 18% and 22%, respectively.[8,21] In addition, and for the R,R′-dialkylimidazolium bis[(trifluoromethyl)sulfonyl]-imide ILs, only surface tension data for $[C_1C_1im][NTf_2]$[8] and $[C_2C_2im][NTf_2]$[21] were found. The average relative deviation between the data collected in this work and the results from literature is 7% and −0.5%, respectively.[8,21] Our data display a lower relative deviation when compared with the surface tension values reported by Carvalho et al.,[21] although measured with a different technique (du Noüy ring method), than those reported by Kolbeck et al.[8] and attained using the pendant drop method. This larger deviation should be a major result of the IL sample and respective purity level and/or water content. In fact, it was already demonstrated that the presence of small amount of impurities or water has a strong impact on the surface tension values.[19] The $[C_1C_1im][NTf_2]$ used by Kolbeck et al.[8] was synthesized by the authors whereas our sample was commercially acquired. Nevertheless, based on the total peak integral in the ^1H NMR spectrum, a purity of 99% was assigned.[8] Therefore, small differences in surface active impurities and water contents (either in the samples used by other authors[8] or in our samples) should be behind the average relative deviation observed.

For all ILs, the surface tension presents a quasi-linear dependence with the temperature as shown in Figures 2 and 3. A regular decrease of the surface tension while increasing the cation side alkyl chain length is observed, and as previously shown experimentally for other IL families,[22−24] reflecting thus the magnitude of the entropy increase associated with the surface assembling. This trend is also extensible to the IL anion (with alkyl(alkenyl)trifluoroborate or carboxylate anions).[25,26] However, this regular decrease is only observed with ILs of limited cation/anion alkyl side chain length. In these situations the force required to break the air/liquid interface is strongly related with the ion−ion interactions.

Later results by Kolbeck et al.[8] and Carvalho et al.[21] revealed that the surface tension values of R-alkyl-3-methylimidazolium bis[(trifluoromethyl)sulfonyl]imide-based ILs (with alkyl chains up to dodecyl) display a regular decrease with the increase on the cation side alkyl chain length only until a critical alkyl chain length size (CACL) of $n = 6$ ($[C_6C_1im][NTf_2]$). For ILs with longer aliphatic moieties the surface tension tends to reach a plateau.[8,21] However, this was previously demonstrated with a limited number of ILs with different alkyl side chain lengths and only for asymmetric ILs (from $[C_2C_1im][NTf_2]$ to $[C_{10}C_1im][NTf_2]$).[21] In this work, and using an extended number of ILs, this behavior is correctly confirmed, as depicted in Figure 4, with a plateau in the surface tension values appearing for ILs with alkyl chains larger than hexyl for both the $[C_nC_1im][NTf_2]$ and $[C_nC_nim][NTf_2]$ series. This behavior is therefore an indication of a change in the surface structuration with the increase of the nonpolar domains as the cation alkyl side chain length increases, and in agreement with the trends observed in the bulk structure

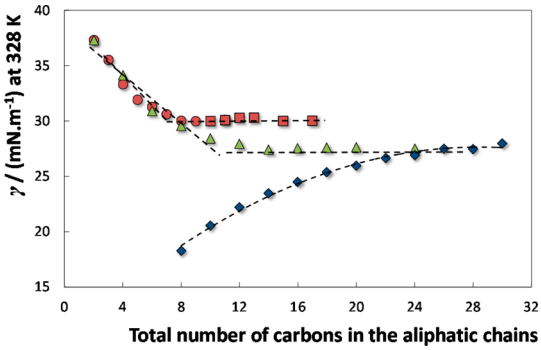

Figure 4. Surface tension dependence, at 328 K, as a function of the total number of carbons in the aliphatic chains: red circle, $[C_nC_1im][NTf_2]$[18] with $n = 1−10$; red square, $[C_nC_1im][NTf_2]$ with $n = 9−16$; green triangle, $[C_nC_nim][NTf_2]$ with $n = 1−12$; blue diamond, *n*-alkanes,[32] C_nH_{2n+2}, with $n = 8−30$.

around $[C_6C_1im][NTf_2]$ either by MD simulations,[27−29] X-ray diffraction studies[30] or by other thermophysical properties,[13] such as density and viscosity. Other works attempted the study of the structure of the gas−liquid and liquid−liquid interfaces of ionic liquids. Lynden−Bell[31] employed MD simulations on the 1,3-dimethylimidazolium chloride evidencing the existence of a region of enhanced number density, and where the vertical alignment of the imidazolium ring allowed the cations to pack more closely. Later on, Lyndell-Bell and Del Pópolo,[32] using three anions combined with the common 1-butyl-3-methyl-imidazolium cation, concluded that the longest butyl side chain tends to face the vacuum whereas the methyl chains are oriented into the liquid. Pensado et al.[33] also employed MD simulations through the liquid-vacuum interface of 1-hexyl-3-methylimidazolium bis(trifluoromethylsulfonyl)amide while calculating several structural properties of the interface, such as the orientational ordering and density profiles. The authors[33] also concluded that the longest hexyl side chain of the imidazolium cation is likely to protrude outward from the surface layer, and that there is a region with enhanced density from that of the bulk where the cation preferably angles with the imidazolium ring and tends to be perpendicular to the interface. Jiang et al.[34] implemented multiscale coarse-grained (MS-CG) MD simulations of the liquid-vacuum interface in room temperature ILs with diverse alkyl side chain lengths. The authors[34] observed that for ILs with long alkyl side chains a multilayer ordering of ions occurs (attributed to the characteristic length scale of nanostructural organization existent in ILs with sufficiently long aliphatic moieties), whereas ILs with a shorter chain exhibit an interfacial structure consistent with a monolayer ordering.

In this work, the bis(trifluoromethylsulfonyl)amide anion is common to all ILs and no major conclusions can be derived from its influence toward the surface ordering. Further works describing the IL anion effect on the surface tensions values and surface ordering can be found elsewhere.[14,35]

Figure 4 depicts the results of surface tension, at 328 K, for $[C_nC_1im][NTf_2]$ (with $n = 2−16$)[18] and $[C_nC_nim][NTf_2]$ (with $n = 1−12$), as well as for *n*-alkanes (C_nH_{2n+2} with $n = 8−30$), as a function of the total number of carbons in the two aliphatic tails. The experimental data for *n*-alkanes were taken from literature[36] and are presented in the Supporting Information in Table SI.3. It should be remarked that the dashed lines presented in Figure 4 (and subsequent figures) have no physical meaning. They are only presented to facilitate

dx.doi.org/10.1021/la501308q | Langmuir 2014, 30, 6408−6418

the reading and to better follow the trendshifts observed. Unlike for ILs, the surface tension of *n*-alkanes increases with the chain length but also displays a tendency toward a stationary value for compounds with a large carbon number. This tendency mirrors the increase of the dispersive forces with the aliphatic chain length. The regular trend observed for the surface tension reflects the isotropic character of the bulk liquid of *n*-alkanes in opposition with the irregular behavior of ILs. In the case of ILs, two distinct and clear regions are observed: a first region, with an accentuated decrease in the surface tension associated with the decrease of the electrostatic interactions, and arising from the increase of the alkyl chain steric hindrance between the ions pairs; a second region, with a stationary surface tension, identical to the long chain length *n*-alkanes, and that is an indication that above the CACL a nonpolar domain of segregated alkyl chain segments will be at the ILs surface. The convergence between the surface tensions of *n*-alkanes and R,R′-dialkylimidazolium-based fluids ($[C_nC_n\text{im}][NTf_2]$) is a strong sign that for long alkyl side chain ILs the surface is mainly made up of aliphatic tails. The alkyl chain interactions will have a major contribution to the surface tension while the polar groups of the ILs have a reduced influence. According to the Langmuir's principle only the parts of the molecule at the outer surface contribute to the surface tension values.[37] On the other hand, the R-alkyl-3-methylimidazolium-based ILs ($[C_nC_1\text{im}][NTf_2]$) reach a plateau with surface tension values higher than that observed in *n*-alkanes or in the R,R′-dialkylimidazolium-($[C_nC_n\text{im}][NTf_2]$) series. This fact suggests that the surface tension of the $[C_nC_1\text{im}][NTf_2]$ series is more affected by the polar domain structuration in the bulk region (responsible for the higher surface tensions observed). The two equivalent aliphatic moieties in $[C_nC_n\text{im}][NTf_2]$ have a huge contribution to predominant van der Waals interactions at the surface, and as such, this symmetric series of ILs resemble *n*-alkanes regarding their surface ordering.

In summary, it is clearly demonstrated here that the surface tensions of imidazolium-based ILs tend to a constant value above a critical alkyl length size that is attained at $[C_6C_1\text{im}][NTf_2]$ and $[C_6C_6\text{im}][NTf_2]$. In addition, the symmetric series of ILs display surface tension values close to *n*-alkanes (for sufficiently long alkyl side chains) indicating that in this type of ILs the surface ordering is mainly defined by the aliphatic tails with a weak contribution of the polar moiety.

The surface thermodynamic properties, namely surface entropy and surface enthalpy, were estimated using the quasi-linear dependence of the surface tension with temperature.[38] The surface entropy, S^γ, was evaluated according to

$$S^\gamma = -\left(\frac{d\gamma}{dT}\right) \tag{1}$$

whereas the surface enthalpy, H^γ, was determined according to

$$H^\gamma = \gamma - T\left(\frac{d\gamma}{dT}\right) \tag{2}$$

where γ stands for the surface tension and T for the temperature.

The values of the thermodynamic functions of all the ILs investigated derived from the temperature dependence of the surface tension, $\gamma = f(T)$, in combination with the associated deviation,[39] are presented in Table SI.4 in the Supporting Information.

The derived surface entropies of the ILs series as well as of the *n*-alkanes are depicted in Figure 5. It should be stressed that

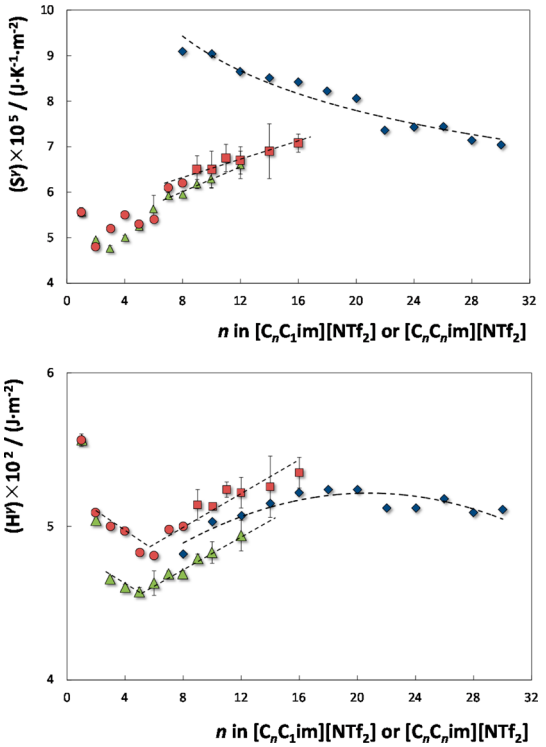

Figure 5. Derived surface entropies and enthalpies at 298 K as a function of the total number of carbon atoms in the aliphatic chains: red circle, $[C_nC_1\text{im}][NTf_2]$[18] with n = 1−8; red square, $[C_nC_1\text{im}][NTf_2]$ with n = 9−16; green triangle, $[C_nC_n\text{im}][NTf_2]$ with n = 1−12; blue diamond, *n*-alkanes,[32] C_nH_{2n+2}, with n = 8−30.

the dashed lines shown in Figure 5 have no physical meaning. For *n*-alkanes, the entropy of surface decreases almost linearly with the increase of the aliphatic tail and which is in agreement with a decrease in the differentiation of the structuration order between the surface and the bulk isotropic region. However, for ILs, an almost general increase in the entropy of surface is found with a stronger increase per methylene group ($-CH_2$) in the short alkyl chain length region. This pattern reflects the effect of the alkyl chain hindrance in the bulk and surface organization of both ILs series. It should be remarked that $[C_1C_1\text{im}][NTf_2]$ is usually an outsider of the general trends due to its higher charge density and low effects exhibited by the two methyl chains. As previously observed for different ILs,[14,21,22,40−42] these fluids exhibit a quite low surface entropy when compared with molecular organic compounds. This evidence reveals a small structural differentiation between the surface and the bulk structured liquid phase in ILs.

As depicted in Figure 5, the entropy of surface for both ILs series converges to the values of *n*-alkanes for a long chain length, and is in agreement with the similarity of surface between ILs and alkanes that would be expected for ILs with long side aliphatic moieties. Furthermore, it is interesting to observe that the entropy of surface seems to be only dependent on the longest alkyl chain length above the CACL, i.e., the derived entropies of surface are similar for $[C_nC_n\text{im}][NTf_2]$ and $[C_nC_1\text{im}][NTf_2]$ at the same value of *n*. The similarity between the entropy of surface for ILs with the same longest alkyl chain length is an indication that the alkyl chain segregation at the

dx.doi.org/10.1021/la501308q | *Langmuir* 2014, 30, 6408−6418

surface seems to involve only one of the aliphatic tails in the $[C_nC_n\text{im}][NTf_2]$ series.

Figure 5 also reveals the surface enthalpies of the several ILs and *n*-alkanes as a function of the number of carbons in the longest alkyl chain. It is observed a decrease on the enthalpy of surface, for both asymmetric and symmetric series of ILs, bellow CACL. After CACL, there is a regular increase on the surface enthalpy. For the asymmetric series of ILs, $[C_nC_1\text{im}][NTf_2]$, the same trend and magnitude on the surface enthalpy was found when compared to *n*-alkanes. This increase is less pronounced in the symmetric series of the type $[C_nC_n\text{im}][NTf_2]$; yet, nearly the same if only the longest alkyl chain is considered. In fact, this pattern is in agreement with the previous discussion on the entropy of surface, and which supports a model of an IL surface that only involves one of the alkyl chains for the $[C_nC_n\text{im}][NTf_2]$ series. The enthalpy of surface is, however, slightly lower for the symmetric $[C_nC_n\text{im}][NTf_2]$ ILs when compared with the asymmetric $[C_nC_1\text{im}][NTf_2]$ for the same size of the longest alkyl chain. Finally, the small difference in the enthalpy of the surface between the two series, in particular for alkyl chains longer than the CALC ($[C_6C_1\text{im}][NTf_2]$ and $[C_6C_6\text{im}][NTf_2]$), appears to rule the observed differentiation in the surface tension results (Figure 4) with higher surface tensions displayed by the asymmetric series ($[C_nC_1\text{im}][NTf_2]$) in the stationary region. This surface organization will be further discussed and supported based on the MD simulation results.

Electrospray ionization mass spectrometry data were also used to gather further insights into the interpretation of the surface tension results. In this context, it was investigated the gas phase fragmentation of isolated $[(C_nC_n\text{im})_2NTf_2]^+$ aggregate ions by collision with a neutral gas (ESI-MS-MS) at variable collision energies. This strategy allows us to infer on the ILs' (cation−anion) interaction energies. The experimental collision energies required to dissociate 50% (as a general reference) of the adduct ion represent the energy required to separate the cation from the neutral IL and, as such, can give an indication of the cation−anion relative strength. The experimental collision energy values are presented in Table SI.5 in the Supporting Information.

The mass spectral data, represented as $E_{cm,1/2}$, are plotted as a function of the total number of carbon atoms in the alkyl side chains of the imidazolium cation, together with surface tension data, in Figure 6. Furthermore, the surface tension data at 328 K as a function of the collision energies are also depicted in Figure 6. In both symmetric and asymmetric series of ILs the variation of the relative cation−anion interactions, expressed by the $E_{cm,1/2}$ values, and the surface tension show a similar trend with the increase of the cation side alkyl chain length. In fact, there is a close correlation between the surface tension of the studied ILs at a common temperature and their relative cation−anion interactions. A more pronounced decrease of the relative cation−anion interaction energy toward an almost constant value for alkyl chains larger than hexyl shows that the length of the alkyl chain (after hexyl) does not induce a significant effect on the predominant Coulombic interactions between the anion and the imidazolium core. This effect is also confirmed by the higher slope displayed between the surface tension and $E_{cm,1/2}$ for alkyl side chains up to hexyl. However, it is observed a slight increase in the energy of interaction from n = 9−12 in the symmetric series of $[C_nC_n\text{im}][NTf_2]$, contrarily to what is observed with the R-alkyl-3-methylimidazolium bis-[(trifluoromethyl)sulfonyl]imide compounds. The contribution

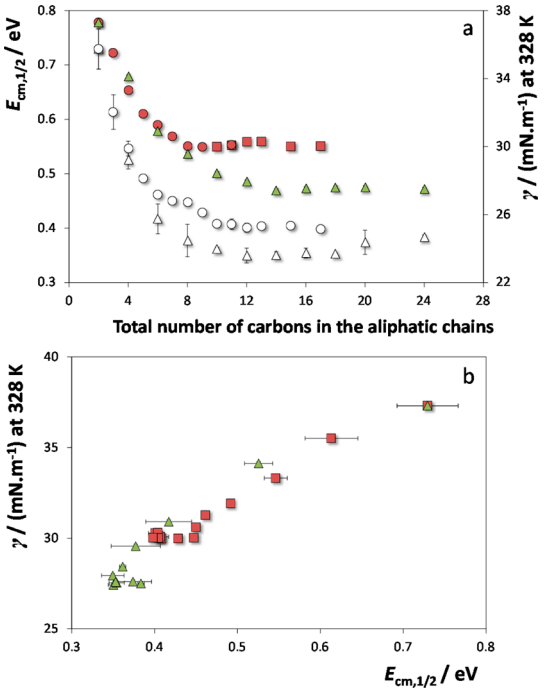

Figure 6. (a) Surface tension at 328 K as a function of the total number of carbons in the aliphatic chains for: red circle, $[C_nC_1\text{im}][NTf_2]$[18] with n = 1−10; red square, $[C_nC_1\text{im}][NTf_2]$ with n = 9−16; green triangle, $[C_nC_n\text{im}][NTf_2]$ with n = 1−12. $E_{cm,1/2}$ values as a function of the total number of carbons in the aliphatic chains for: white circle, $[C_nC_1\text{im}][NTf_2]$[15] with n = 1−16; white triangle, $[C_nC_n\text{im}][NTf_2]$ with n = 1−12. (b) Surface tension at 328 K as a function of $E_{cm,1/2}$ for: red square, $[C_nC_1\text{im}][NTf_2]$;[15,18]; green triangle, $[C_nC_n\text{im}][NTf_2]$ with n = 1−12.

of stronger van der Waals interactions between the two alkyl chains, for the symmetric cations, which are absent in the asymmetric ones, is a plausible explanation for these observations.

The close relationship between surface tension and cation−anion relative interaction energies, shown in Figure 6, indicates that the relative orientation of the cations and anions at the surface is also a reflection of the cohesive forces between the ions occurring at the bulk which, on the other hand, will become practically independent of the length of the alkyl side chain for higher values of *n*.

The structure of the IL at the vacuum-liquid interface was further explored using Molecular Dynamics simulation data. Extensive simulation runs (cf. Experimental Section) of the pure $[C_{10}C_{10}\text{im}][NTf_2]$ IL in an isotropic bulk and in a setup comprising an IL slab with two free surfaces allowed us to probe the distinctive behavior of the two alkyl side chains of the imidazolium cations when approaching the surface. The results are summarized in Figure 7.

Figure 7a depicts the number density profiles of three selected types of atom of the $[C_{10}C_{10}\text{im}][NTf_2]$ IL along the normal direction to the free surface planes. The three chosen atoms selectively probe the position of the end of the alkyl side chains (where CT are the terminal carbon atoms of the alkyl side chains), the position of the anions (where NBT is the nitrogen atom of the $[NTf_2]$ ion) and the position of the charged part of the cation (CR is the carbon atom between the two nitrogen atoms of the imidazolium ring). As shown previously by other authors,[33] as one approaches the surface

dx.doi.org/10.1021/la501308q | *Langmuir* 2014, 30, 6408−6418

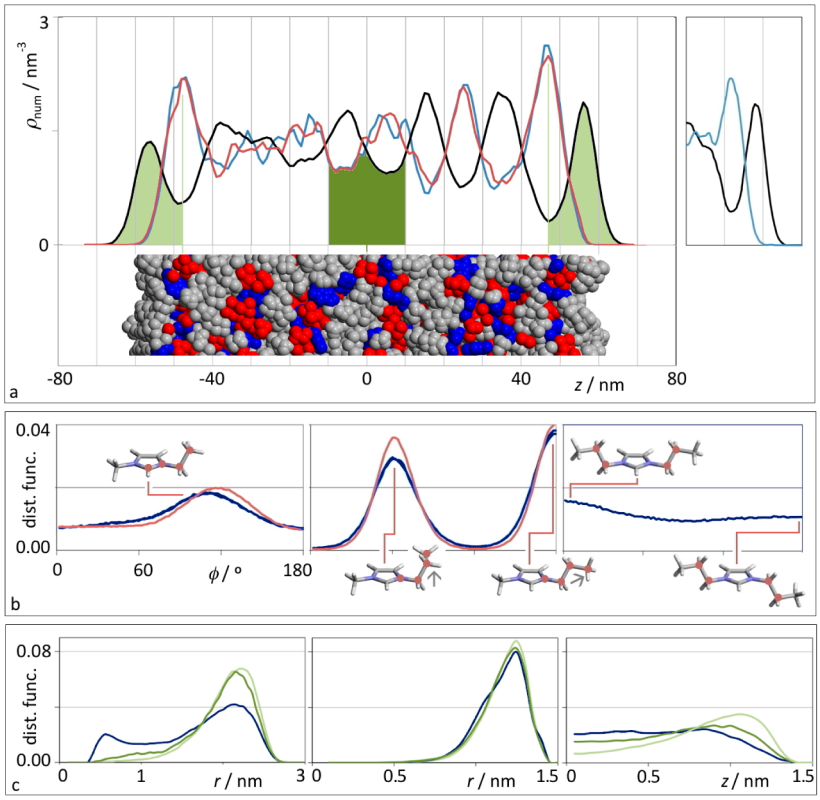

Figure 7. (a) Numerical density profiles, ρ_{num}, along the direction normal to the surfaces, z, for three selected atom types in $[C_{10}C_{10}im][NTf_2]$: chain terminal carbon atoms, CT (black lines); nitrogen atom of the anion (red lines); imidazolium ring centroid, im (blue lines). The image on the top right shows the same distribution for $[C_6C_1im][Ntf_2]$. The green areas mark the outermost nonpolar surface layers (light) and the central region of the slab (dark). The partial simulation snapshot was scaled and positioned in the same z-scale in order to highlight the two free surfaces. The ions are depicted as red (anions), blue (charged parts of the cations), and gray (chains from C2 to C10). (b) Probability distribution functions for three dihedral angles in bulk $[C_{10}C_iim]^+$. Blue lines represent data for $[C_{10}C_{10}im][NTf_2]$ and the red lines for $[C_{10}C_1im][NTf_2]$. The molecular structures show the most probable conformations of a given dihedral angle given by the four atoms highlighted in red. (c) Probability distribution functions of the CT−CT distance (left), CT−im distances (middle), and CT−im z-projected distances (right). The blue lines correspond to bulk $[C_{10}C_{10}im][NTf_2]$, the light and dark green lines to the two areas (outermost and central) of the IL slab depicted in panel a.

from the vacuum sides, the first layer to be found is composed of the alkyl side chain(s) of the cation. This is immediately followed by a (polar) layer enriched in the charged parts of the ions that compose the IL (the imidazolium ring and the atoms directly attached to it and the bistriflamide anion). The main difference between the system under discussion with the symmetrically substituted cations and previous atomistic simulations with a single (albeit smaller) alkyl chain is that in the former example the polar layer is followed by a second well-defined layer enriched in alkyl side chains, whereas in the latter cases such secondary nonpolar layer is almost absent (cf. image on the right of panel a).[33] This seems to endorse the hypothesis previously formulated suggesting that in most cases one of the two alkyl chains of the cations point toward the surface while the second points in the opposite direction (and swells the ranks of this secondary nonpolar layer). The numerical density profiles also show that this layering continues to be noticeable further away from the free surfaces (alternation between chain-rich and polar-head-rich layers). This kind of situation has been previously observed in coarse-grained simulations of single-chained cations (10 or 12 carbon atoms long chains) combined with small and rigid anions.[34] However, it must be pointed out that the thickness of the present IL slab (only 10 nm) may cause spurious interference effects caused by the proximity of the two surfaces, including the asymmetry of the generated density profiles. Nevertheless, the structural effects at distances close to the two surfaces are clear and enable further analyses centered in the relations between the structure of the outermost layers and surface tension.

To further analyze the relative orientation of the two chains of a given cation at the surface, we have first checked which are the most probable conformations adopted by the two aliphatic chains around the imidazolium ring. Figure 7b shows relevant dihedral angle distributions along the chains in single- and symmetrically chained imidazolium rings. The distribution profiles show that (i) the conformations adopted by a given chain in a single or symmetrically substituted cation are almost equivalent (cf. blue and red lines) revealing that in the latter case the two chains can adopt conformations that, barring possible overlaps, are independent of the conformation adopted by the other; (ii) the first carbon atom along the chains that is able to move outside the plane of the imidazolium ring (C2) prefers to adopt nonplanar conformations (left image in Figure 7b), however, other conformations, including planar ones, also have a relatively high probability of existence; (iii) the third carbon (C3) can choose from two almost equivalent positions, generally dubbed anti and gauche[43] (middle image in Figure 7b); (iv) from C4 onward the chains behave like normal alkyl chains and prefer to adopt anti (zigzag) conformations. Depending on the conformation at the C3 carbon, this has the effect of obtaining stretched chains that are oriented almost perpendicular to the plane of the ring (gauche at C3, vertical

dx.doi.org/10.1021/la501308q | Langmuir 2014, 30, 6408−6418

arrow in the middle image of panel b of Figure 7) or not in the plane of the ring but away from it (anti at C3, slanted arrow in the middle image of panel b); and (v) when two chains are present, the relative orientation of their C2 carbons (the way the chains leave the ring relative to each other) show a very shallow probability distribution function, right image of panel b of Figure 7, with a slightly larger probability of the chains leaving the ring on the same side.

This state of affairs confirms the existence of all conformations of symmetrically substituted imidazolium cations, found in the corresponding IL crystals,[44] also in their liquid sate: the so-called U-conformations (chains parallel to each other and side by side) occur when both chains leave to the same side and both adopt gauche conformations at C3; V-conformations (not parallel to each other) occur when the chains are gauche-anti at C3 or both chains leave from the same side of the ring and are anti−anti at C3; and I-conformations (chains parallel to each other but not side by side) occur when the chains leave on opposite sides of the ring and are both anti or gauche at C3. In the bulk liquid, all these conformations are able to coexist and can easily interconvert into each other.

Given the possibility of such conformational freedom in the bulk, the final issue to be discussed is the influence of the structuration (layering) at the surface on the conformations of the cations and the possibility of pointing both or just one of its aliphatic chains toward the free surface.

Figure 7a allows the estimation of the average number of tails that are at the surface —all terminal carbon atoms of the chain that are found correspond to the light green areas. In the present simulations, this corresponds to averages of 62.5 and 54.9 tails at those two nonpolar surface layers. Some of these tails belong to the same cation but since all tails are indexed to the ions it is straightforward to calculate the number of distinct cations that have at least one aliphatic chain at the surface. This yields 44.8 and 41.3 for the two surfaces. This means that 17.7 (= 62.5−44.8) and 13.6 (= 54.9−41.3) cations have both tails at the surface while the rest (27.1 and 27.7) have one tail pointing toward the surface and the other away from it. Thus, the model supports the idea that, at the outermost polar layers, more cations point one of their tails outward and the other inward relative to the surface than cations pointing both tails outward. The number of the former exceeds the number of the latter by about 75%.

Finally, Figure 7c shows that while in bulk $[C_{10}C_{10}im][NTf_2]$ some cations adopt U-conformations with modest distances between the two CT atoms (blue line in the left image of Figure 7c), in the IL slab (dark and green lines) such conformations are suppressed, specially for the outermost layers. On the other hand, the central image of Figure 7c shows that the im-CT distances in the bulk or in the layered systems are very similar and correspond to a fair proportion of completely stretched (zigzag) chains. However, if projections of these distances are made in the z direction (or in an arbitrary axis in the bulk system), one observes that the chains closer to the surface tend to adopt orientations more perpendicular to it (right image of Figure 7c). It must be stressed that this distance analysis can be performed independently of the relative number of U, V or I conformers present in the bulk and surface layers (which, as seen in Figure 7b, do not differ so much).

The development of quantitative structure−property relationships and predictive methods for ILs is an important topic in the characterization of these fluids as well as to estimate their thermophysical properties when no experimental data are available. The Larriba et al.[45] model, based on the cavity theory, was a pioneering work correlating the surface tension and void fraction in ILs. The void fraction considers the difference between the liquid volume occupied by an ion pair (known from cationic and anionic weights and liquid density measurements) and the sum of the ionic volumes (known from crystal structures). Later, Gardas and Coutinho[46] proposed a quantitative structure−property correlation for the estimation of the surface tension of ILs based on parachors and density data and/or their molar volumes. The dependency of the surface tension as a function of the molar volume for $[C_nC_1im][NTf_2]$ (n = 1−16), $[C_nC_nim][NTf_2]$ (n = 1−12) and n-alkanes (n = 8−30) is depicted in Figure SI.1 in the Supporting Information. The molar volumes of ILs and n-alkanes were obtained from density data at 328.15 K taken from literature.[13,36,47−49] The general trend obtained clearly suggests that, for ILs with small alkyl side chains, the molar volumes have an influence on the surface tension, which, for longer alkyl chains in $[C_nC_nim][NTf_2]$ and n-alkanes stabilizes at approximately the same molar volume.

The determination of the triple and critical points of a given substance allows the characterization of its pressure−temperature liquid range in addition to the indication of the boundaries of the corresponding liquid−gas equilibrium curve. The critical temperature, T_c, is a recurrent property commonly used in corresponding states correlations describing equilibrium and transport properties.[50] Nevertheless, the experimental determination of the critical temperatures of ILs is a challenging task since they decompose before reaching their critical temperature. Rebelo et al.[20] proposed the use of the Eötvos[51] and Guggenheim[52] equations to estimate the critical temperature of ILs according to

$$\gamma\left(\frac{M}{\rho}\right)^{(2/3)} = K(T_c - T) \tag{3}$$

$$\gamma = K\left(1 - \frac{T}{T_c}\right)^{(11/9)} \tag{4}$$

where T_c is the critical temperature, M is the molecular weight, ρ is the density, and K is a fitting parameter.

Both equations reflect the fact that the surface tension becomes null at the critical point. The critical temperature values estimated from the surface tension data obtained in this work are reported in Table SI.4 in Supporting Information. The estimation of critical temperatures using surface tension data from a restricted temperature range can introduce an important source of error and it should be highlighted that these values must be used with caution. On the other hand, Rai and Maggin[53] already showed that the critical temperatures estimated by these simple methods are in good agreement with those obtained by molecular simulation calculations and, at least, can provide a support for the observed patterns. Nevertheless, due to the inherent difference on both approaches (experimental results versus MD simulation), different values will be inevitably obtained. The major agreement is found on trends and not on the absolute values of surface tension when analyzing, for instance, the $[C_nmim][NTf_2]$ series of ILs.

The critical temperature values are depicted in Figure 8, for both the asymmetric and symmetric ILs and n-alkanes. With the exception of the $[C_1C_1im][NTf_2]$, which is an outlier to

dx.doi.org/10.1021/la501308q | Langmuir 2014, 30, 6408−6418

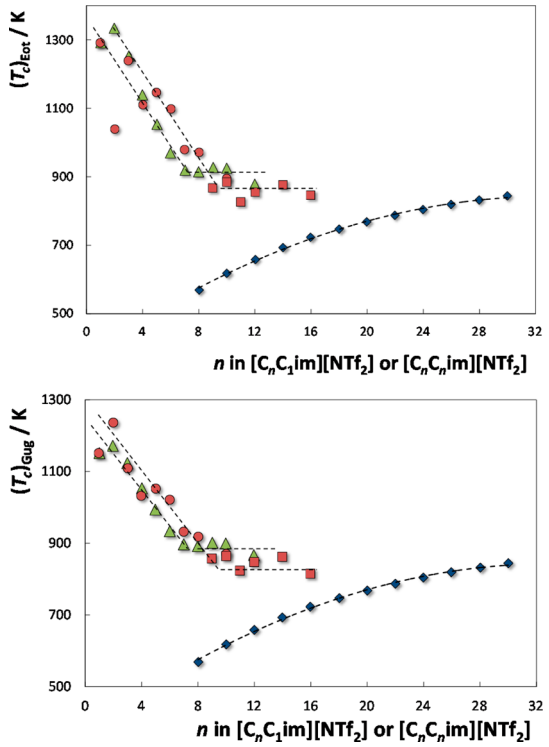

Figure 8. Estimated critical temperatures, using the Eötvos $((T_c)_{Eot})$[45] and Guggenheim $((T_c)_{Gug})$[46] equations as a function of the total number of carbon atoms in the aliphatic chains: red circle, $[C_nC_1im][NTf_2]$[18] with n = 1−10; red square, $[C_nC_1im][NTf_2]$ with n = 9−16; green triangle, $[C_nC_nim][NTf_2]$ with n = 1−12; blue diamond, n-alkanes,[32] C_nH_{2n+2}, with n = 8−30.

this trend, a steep decrease in the critical temperatures is observed until n = 7, after which the critical temperatures decrease more slowly and appear to converge to those of the n-alkanes. A similar trend is observed for R-alkyl-3-methylimidazolium bis[(trifluoromethyl)sulfonyl]imide ILs. The two approaches used reveal similar trends for the critical temperature as a function of the number of carbon atoms in the longest aliphatic tail. As for the surface tension values discussed above, it seems that for long chain ILs, the alkyl moiety becomes dominant in the compound properties and the IL critical temperatures approaches those of n-alkanes of similar chain length.

CONCLUSIONS

New experimental data were reported for the surface tension of two extended series of symmetric and asymmetric ILs, namely $[C_nC_nim][NTf_2]$ and $[C_nC_1im][NTf_2]$. The surface tension values were determined in the temperature range from (298 to 343) K and at atmospheric pressure. In both series, the surface tensions decrease with increasing the alkyl chain length up to a CACL that occurs at hexyl. For aliphatic tails longer than hexyl, either in $[C_6C_6im][NTf_2]$ or $[C_6C_1im][NTf_2]$, the surface tensions reach an almost constant value up to $[C_{12}C_{12}im]$-$[NTf_2]$ and $[C_{16}C_1im][NTf_2]$. The same trend was found in the relative cation−anion interaction energies measured by mass spectrometry pointing out to the importance of the cohesive forces in the surface organization of ILs. In addition, the surface tensions of $[C_nC_nim][NTf_2]$ converge to those displayed by n-alkanes providing novel evidence on the surface ordering of this type of fluids that is essentially made up of aliphatic moieties. On the other hand, the surface tensions of the asymmetric series are always higher reflecting the effect of the stronger contribution of the polar interaction in the bulk ILs. The similarity between the entropy of surface for both ILs series (with the same longest alkyl side chain length) is proposed as an indication that the alkyl chain segregation at the surface involves mostly one of the aliphatic tails in the $[C_nC_nim][NTf_2]$ series. In-between the two series it was further found that the enthalpy of surface rules the observed differentiation in the surface tension in the stationary region (after CACL). An analysis at the molecular scale using Molecular Dynamics simulation data corroborates the experimental surface tension results and the surface organization model proposed.

The hypothetical critical temperatures of the ILs investigated were also estimated. The critical temperatures converge to those of n-alkanes, with a similar alkyl chain length, providing therefore additional evidence that the aliphatic tails also dominate the behavior of these properties in sufficiently long alkyl chain ionic fluids.

The information provided in this work is particularly useful in the understanding of the cation alkyl side chain length and symmetry effects through the surface ordering of ILs, which was hitherto poorly understood.

ASSOCIATED CONTENT

Supporting Information

Water content in the several ILs, surface tension of ILs and n-alkanes, surface thermodynamic functions, estimated critical temperatures, and experimental collision energies required to dissociate 50% of the adduct ion determined by ESI-MS-MS spectra. This material is available free of charge via the Internet at http://pubs.acs.org.

AUTHOR INFORMATION

Corresponding Author

*E-mail: jcoutinho@ua.pt. Tel: +351-234-370200. Fax: +351-234-370084.

Notes

The authors declare no competing financial interest.

ACKNOWLEDGMENTS

This work was financed by QREN SI−I&DT Project 11551 from UE/FEDER through COMPETE program. The authors also acknowledge FCT-*Fundação para a Ciência e a Tecnologia* for the projects Pest-C/CTM/LA0011/2013, PEst-OE/QUI/UI0100/2013, FCT-ANR/CTM-NAN/0135/2012 (including a postdoctoral grant of KS), PTDC/CTM-NAN/121274/2010 and PTDC/QUI-QUI/121520/2010. P.M. acknowledges the postdoctoral grant SFRH/BPD/81748/2011.

REFERENCES

(1) Seddon, K. R. Ionic liquids: A taste of the future. *Nat. Mater.* **2003**, *2*, 363−365.

(2) Welton, T. Room-Temperature Ionic Liquids. Solvents for Synthesis and Catalysis. *Chem. Rev.* **1999**, *99*, 2071−2084.

(3) Gaune-Escard, M.; Seddon, K. R.: Molten salts and ionic liquids: never the twain? John Wiley: Hoboken, N.J., 2010.

(4) Rogers, R. D.; Seddon, K. R. Ionic Liquids - Solvents of the Future? *Science* **2003**, *302*, 792−793.

(5) Conceição, L. J. A.; Bogel-Lukasik, E.; Bogel-Lukasik, R. A new outlook on solubility of carbohydrates and sugar alcohols in ionic liquids. *RSC Adv.* **2012**, *2*, 1846−1855.

(6) Wang, H.; Gurau, G.; Rogers, R. D. Ionic liquid processing of cellulose. *Chem. Soc. Rev.* **2012**, *41*, 1519−1537.
(7) Plechkova, N. V.; Seddon, K. R. Applications of ionic liquids in the chemical industry. *Chem. Soc. Rev.* **2008**, *37*, 123−150.
(8) Kolbeck, C.; Lehmann, J.; Lovelock, K. R. J.; Cremer, T.; Paape, N.; Wasserscheid, P.; Fröba, A. P.; Maier, F.; Steinrück, H. P. Density and Surface Tension of Ionic Liquids. *J. Phys. Chem. B* **2010**, *114*, 17025−17036.
(9) Law, G.; Watson, P. R. Surface Tension Measurements of N-Alkylimidazolium Ionic Liquids. *Langmuir* **2001**, *17*, 6138−6141.
(10) Tariq, M.; Freire, M. G.; Saramago, B.; Coutinho, J. A. P.; Lopes, J. N. C.; Rebelo, L. P. N. Surface tension of ionic liquids and ionic liquid solutions. *Chem. Soc. Rev.* **2012**, *41*, 829−868.
(11) Oliveira, F. S.; Freire, M. G.; Carvalho, P. J.; Coutinho, J. A. P.; Lopes, J. N. C.; Rebelo, L. P. N.; Marrucho, I. M. Structural and Positional Isomerism Influence in the Physical Properties of Pyridinium NTf_2-Based Ionic Liquids: Pure and Water-Saturated Mixtures. *J. Chem. Eng. Data* **2010**, *55*, 4514−4520.
(12) Freire, M. G.; Neves, C. M. S. S.; Shimizu, K.; Bernardes, C. E. S.; Marrucho, I. M.; Coutinho, J. A. P.; Lopes, J. N. C.; Rebelo, L. P. N. Mutual Solubility of Water and Structural/Positional Isomers of N-Alkylpyridinium-Based Ionic Liquids. *J. Phys. Chem. B* **2010**, *114*, 15925−15934.
(13) Rocha, M. A. A.; Neves, C. M. S. S.; Freire, M. G.; Russina, O.; Triolo, A.; Coutinho, J. A. P.; Santos, L. M. N. B. F. Alkylimidazolium Based Ionic Liquids: Impact of Cation Symmetry on Their Nanoscale Structural Organization. *J. Phys. Chem. B* **2013**, *117*, 10889−10897.
(14) Almeida, H. F. D.; Lopes-da-Silva, J. A.; Freire, M. G.; Coutinho, J. A. P. Surface tension and refractive index of pure and water-saturated tetradecyltrihexylphosphonium-based ionic liquids. *J. Chem. Thermodyn.* **2013**, *57*, 372−379.
(15) Fernandes, A. M.; Rocha, M. A. A.; Freire, M. G.; Marrucho, I. M.; Coutinho, J. A. P.; Santos, L. M. N. B. F. Evaluation of Cation−Anion Interaction Strength in Ionic Liquids. *J. Phys. Chem. B* **2011**, *115*, 4033−4041.
(16) Canongia Lopes, J. N.; Deschamps, J.; Pádua, A. A. H. Modeling ionic liquids using a systematic all-atom force field. *J. Phys. Chem. B* **2004**, *108*, 2038−2047.
(17) Canongia Lopes, J. N.; Pádua, A. A. H. Molecular Force Field for Ionic Liquids Composed of Triflate or Bistriflylimide Anions. *J. Phys. Chem. B* **2004**, *108*, 16893−16898.
(18) Smith, W.; Forester, T. R. *The DL_POLY Package of Molecular Simulation Routines (v.2.2)*; The Council for The Central Laboratory of Research Councils; Daresbury Laboratory: Warrington, U.K., 2006.
(19) Tariq, M.; Serro, A. P.; Mata, J. L.; Saramago, B.; Esperança, J. M. S. S.; Canongia Lopes, J. N.; Rebelo, L. P. N. High-temperature surface tension and density measurements of 1-alkyl-3-methylimidazolium bistriflamide ionic liquids. *Fluid Phase Equilib.* **2010**, *294*, 131−138.
(20) Rebelo, L. P. N.; Canongia Lopes, J. N.; Esperança, J. M. S. S.; Filipe, E. On the Critical Temperature, Normal Boiling Point, and Vapor Pressure of Ionic Liquids. *J. Phys. Chem. B* **2005**, *109*, 6040−6043.
(21) Carvalho, P. J.; Freire, M. G.; Marrucho, I. M.; Queimada, A. J.; Coutinho, J. A. P. Surface tensions for the 1-Alkyl-3-methylimidazolium bis(trifluoromethylsulfonyl)imide ionic liquids. *J. Chem. Eng. Data* **2008**, *53*, 1346−1350.
(22) Freire, M. G.; Carvalho, P. J.; Fernandes, A. M.; Marrucho, I. M.; Queimada, A. J.; Coutinho, J. A. P. Surface Tensions of Imidazolium Based Ionic Liquids: Anion, Cation, Temperature and Water Effect. *J. Colloid Interface Sci.* **2007**, *314*, 621−630.
(23) Dzyuba, S. V.; Bartsch, R. A. Influence of Structural Variations in 1-Alkyl(aralkyl)-3-Methylimidazolium Hexafluorophosphates and Bis(trifluoromethylsulfonyl)imides on Physical Properties of the Ionic Liquids. *ChemPhysChem* **2002**, *3*, 161−166.
(24) Law, G.; Watson, P. R. Surface orientation in ionic liquids. *Chem. Phys. Lett.* **2001**, *345*, 1−4.
(25) Zhou, Z.-B.; Matsumoto, H.; Tatsumi, K. Structure and Properties of New Ionic Liquids Based on Alkyl- and Alkenyltrifluoroborates. *ChemPhysChem* **2005**, *6*, 1324−1332.
(26) Xu, A.; Wang, J.; Zhang, Y.; Chen, Q. Effect of Alkyl Chain Length in Anions on Thermodynamic and Surface Properties of 1-Butyl-3-methylimidazolium Carboxylate Ionic Liquids. *Ind. Eng. Chem. Res.* **2012**, *51*, 3458−3465.
(27) Pádua, A. A. H.; Costa Gomes, M. F.; Canongia Lopes, J. N. A. Molecular Solutes in Ionic Liquids: A Structural Perspective. *Acc. Chem. Res.* **2007**, *40*, 1087−1096.
(28) Shimizu, K.; Bernardes, C. E. S.; Canongia Lopes, J. N. Structure and Aggregation in the 1-Alkyl-3-Methylimidazolium Bis-(trifluoromethylsulfonyl)imide Ionic Liquid Homologous Series. *J. Phys. Chem. B* **2014**, *118*, 567−576.
(29) Santos, L. M. N. B. F.; Canongia Lopes, J. N.; Coutinho, J. A. P.; Esperança, J. M. S. S.; Gomes, L. R.; Marrucho, I. M.; Rebelo, L. P. N. Ionic Liquids: First Direct Determination of their Cohesive Energy. *J. Am. Chem. Soc.* **2007**, *129*, 284−285.
(30) Olga, R.; Alessandro, T.; Lorenzo, G.; Ruggero, C.; Dong, X.; Larry, G. H., Jr.; Richard, A. B.; Edward, L. Q.; Natalia, P.; Kenneth, R. S. Morphology and intermolecular dynamics of 1-alkyl-3-methylimidazolium bis{(trifluoromethane)sulfonyl}amide ionic liquids: structural and dynamic evidence of nanoscale segregation. *J. Phys.: Condens. Matter* **2009**, *21*, 424121.
(31) Lynden-Bell, R. M. Gas-liquid interfaces of room temperature ionic liquids. *Mol. Phys.* **2003**, *101*, 2625−2633.
(32) Lynden-Bell, R. M.; Pópolo, M. G. D. Simulation of the surface structure of butylmethylimidazolium ionic liquids. *Phys. Chem. Chem. Phys.* **2006**, *8*, 949−954.
(33) Pensado, A. S.; Malfreyt, P.; Pádua, A. H. A. Molecular Dynamics Simulations of the Liquid Surface of the Ionic Liquid 1-Hexyl-3-methylimidazolium Bis(trifluoromethanesulfonyl)amide: Structure and Surface Tension. *J. Phys. Chem. B* **2009**, *113*, 14708−14718.
(34) Jiang, W.; Wang, Y.; Yan, T.; Voth, G. A. A Multiscale Coarse-Graining Study of the Liquid/Vacuum Interface of Room-Temperature Ionic Liquids with Alkyl Substituents of Different Lengths. *J. Phys. Chem. C* **2008**, *112*, 1132−1139.
(35) Almeida, H. F. D.; Teles, A. R. R.; Lopes-da-Silva, J. A.; Freire, M. G.; Coutinho, J. A. P. Influence of the Anion on the Surface Tension of 1-ethyl-3-methylimidazolium-based Ionic Liquids. *J. Chem. Thermodyn.* **2012**, *54*, 49−54.
(36) Data from DIADEM Public 1.2.
(37) Langmuir, I. Forces Near the Surfaces of Molecules. *Chem. Rev.* **1930**, *6*, 451−479.
(38) Adamson, A. W.; Gast, A. P. *Physical Chemistry of Surfaces*; John Wiley: New York, 1997.
(39) Miller, J. C.; Miller, J. N. *Statistics for Analytical Chemistry*. PTR Prentice Hall: Chichester, U.K.,1993.
(40) Ghatee, M. H.; Bahrami, M.; Khanjari, N. Measurement and study of density, surface tension, and viscosity of quaternary ammonium-based ionic liquids ($[N_{222(n)}]Tf_2N$. *J. Chem. Thermodyn.* **2013**, *65*, 42−52.
(41) Bittner, B.; Wrobel, R. J.; Milchert, E. Physical properties of pyridinium ionic liquids. *J. Chem. Thermodyn.* **2012**, *55*, 159−165.
(42) Xu, W.-G.; Li, L.; Ma, X.-X.; Wei, J.; Duan, W.-B.; Guan, W.; Yang, J.-Z. Density, Surface Tension, and Refractive Index of Ionic Liquids Homologue of 1-Alkyl-3-methylimidazolium Tetrafluoroborate $[C_nmim][BF_4]$ (n = 2,3,4,5,6). *J. Chem. Eng. Data* **2012**, *57*, 2177−2184.
(43) Canongia Lopes, J. N. A.; Pádua, A. A. H. Using Spectroscopic Data on Imidazolium Cation Conformations To Test a Molecular Force Field for Ionic Liquids. *J. Phys. Chem. B* **2006**, *110*, 7485−7489.
(44) Wang, X.; Vogel, C. S.; Heinemann, F. W.; Wasserscheid, P.; Meyer, K. Solid-State Structures of Double-Long-Chain Imidazolium Ionic Liquids: Influence of Anion Shape on Cation Geometry and Crystal Packing. *Cryst. Growth Des.* **2011**, *11*, 1974−1988.

(45) Larriba, C.; Yoshida, Y.; Fernández de la Mora, J. Correlation between Surface Tension and Void Fraction in Ionic Liquids. *J. Phys. Chem. B* **2008**, *112*, 12401−12407.
(46) Gardas, R. L.; Coutinho, J. A. P. Applying a QSPR correlation to the prediction of surface tensions of ionic liquids. *Fluid Phase Equilib.* **2008**, *265*, 57−65.
(47) Gardas, R. L.; Freire, M. G.; Carvalho, P. J.; Marrucho, I. M.; Fonseca, I. M. A.; Ferreira, A. G. M.; Coutinho, J. A. P. *PρT* Measurements of Imidazolium-Based Ionic Liquids. *J. Chem. Eng. Data* **2007**, *52*, 1881−1888.
(48) Esperança, J. M. S. S.; Visak, Z. P.; Plechkova, N. V.; Seddon, K. R.; Guedes, H. J. R.; Rebelo, L. P. N. Density, Speed of Sound, and Derived Thermodynamic Properties of Ionic Liquids over an Extended Pressure Range. 4. $[C_3mim][NTf_2]$ and $[C_5mim][NTf_2]$. *J. Chem. Eng. Data* **2006**, *51*, 2009−2015.
(49) Gomes de Azevedo, R.; Esperança, J. M. S. S.; Szydlowski, J.; Visak, Z. P.; Pires, P. F.; Guedes, H. J. R.; Rebelo, L. P. N. Thermophysical and thermodynamic properties of ionic liquids over an extended pressure range: $[bmim][NTf_2]$ and $[hmim][NTf_2]$. *J. Chem. Thermodyn.* **2005**, *37*, 888−899.
(50) Poling, B. E.; Prausnitz, J. M.; O'Connell, J. P. *The Properties of Gases and Liquids*; McGraw-Hill: New York, 2001.
(51) Shereshefsky, J. L. Surface tension of saturated vapors and the equation of eotvos. *J. Phys. Chem.* **1931**, *35*, 1712−1720.
(52) Guggenheim, E. A. The Principle of Correspondig States. *J. Chem. Phys.* **1945**, *13*, 253−261.
(53) Rai, N.; Maginn, E. J. Vapor−Liquid Coexistence and Critical Behavior of Ionic Liquids via Molecular Simulations. *J. Phys. Chem. Lett.* **2011**, *2*, 1439−1443.